(1) Comments from Referee #1

This is an interesting work to explore the interconnections among different climate modes. They found there are four basic periods in different climate indices, whereas the other periods can be taken as the harmonics of these four basic periods. There are some issues should be well addressed before the acceptance of this submission. First of all, for the same climate mode, such as NAO, different indices reach different period results (see Fig. 2), why? The authors should provide their explanations to these differences. Secondly, for the common basic periods to all studied climate indices, the physical implications should be provided. Thirdly, the peak values for each period are given, how about their uncertainties?

(2) Author's response

Thank you for your encouraging comments.

We sincerely appreciate this helpful and insightful comments and the corrections to English that you have provided. Basically, there are three comments: 1) why the difference between NAO and NAOI in fig. 2; 2) what are the physics here, and 3) what are the uncertainties in the peak values. Comments 1 and 2 are related and we will discuss them together.

Comments 1 and 3

The definitions of two NAO indices we used in this study are different. One is defined as the difference in monthly atmospheric pressures between two action centers in Iceland and Azores during 1825-2017. Another observationally-based monthly NAO index for the period of 1850-2015 (referred to as NAOI) is defined as the difference in the normalized sea level pressures (SLP) that are zonally-averaged over the North Atlantic sector from 80°W to 30°E between 35°N and 65°N. NOAI is derived from the HadSLP dataset with the base period of 1961-1990.

Figure 2, is an illustration for an embedding dimension to 13 to detect the peak-periods of the driving factors of NAO (SFA-NAO) and NAOI (SFA-NAOI). These results suggest that the peak-periods of SFA-NAO are related to ENSO and solar activities, and the peak periods of SFA-NAOI are associated with ENSO, QBO and solar activities (see Figure 2 and Figure 3). However, as Figure 3 shows, when we vary the embedding dimensions from 1 to 25, the peak-periods of both SFA-NAO and SFA-NAOI show robust relations with ENSO, QBO and solar activities. In a way, repeating for many embedding dimensions serves as a sensitivity analysis to see if the results are robust. To further demonstrate this we present some arguments based on a simple known system.

In this study, we did not quantify the uncertainties of the peak values. Here, we use an ideal model to show the change of the significant peak periods of SFA-derived signals among different embedding dimensions. Results show that the peak periods of SFA signal are enough to represent the characteristics of the driving force factors, either the combination of the independent driving force factors or only the slowest driving force factor. Sensitive test of SFA with different embedding dimensions is an effective way to exacting the information of driving force factors.

Consider a logistic map with two-level structures which contains two driving time-varying factors a(t) and b(t):

$$x(t+1) = a(t)x(t)(b(t) - x(t)), (t = 1,2,\ldots,n) \quad \ldots(1)$$

Where

$$a(t) = 3.5 + 0.4\cos(2pt/78) \quad \ldots(2)$$

$$b(t) = 0.998 + 0.024\cos(2p^2t/78) \quad \ldots(3)$$

From formulas (2) and (3), we can compute the true periods of a(t) and b(t) are nearly 78.00 and 24.84 steps, respectively.

First, we set the embedding dimension m to 6 for the SFA and extract the driving-force signal from x(t), which is denoted as sfa-x(t).

Figure 1s a and 1s b below show the time series of the parameters (a(t) and b(t)) in the Logistic map with two-level structure. Figure 1s c shows the non-stationary time series x(t), which is controlled by a(t) and b(t). The driving signal of x(t) when setting embedding dimension m to be 6 (i.e. sfa-x(t)) is shown in Figure 1s d. From Figure 1s, we can see that the temporal evolution of sfa-x(t) is neither a(t) or b(t), but the combination form of them. As a result, we can detect the driving information of sfa-x(t) robustly through wavelet analysis. Figure 2s shows the time-averaged power spectrum of each parameter in Figure 1s. We can see that the significant peak periods in Figure 2s a and Figure 2s b are very close to the true period of a(t) and b(t). The significant peak periods of sfa-x(t) are equal to the significant peak periods of a(t) and b(t). It means that the significant peak periods of SFA-derived signals represent the periodic characteristics of detected driving forces very well. As we mentioned above, only one embedding dimension is not enough to demonstrate the effectiveness of SFA. To reconfirm the results derived from SFA and wavelet analysis, we carry out a series of sensitivity tests to identify the significant peak periods of SFA-derived signals by setting the embedding dimensions from 2 to 16. The peak periods in the time-averaged power spectrum of SFA signals (significant at a significance level of 0.05) with different embedding dimensions are shown in Figure 3s. Results show that under different embedding dimension, SFA signal is ether the combination of different independent driving force factor, or

only the slowest driving force factor (higher embedding dimensions tend to smooth out the faster oscillations).

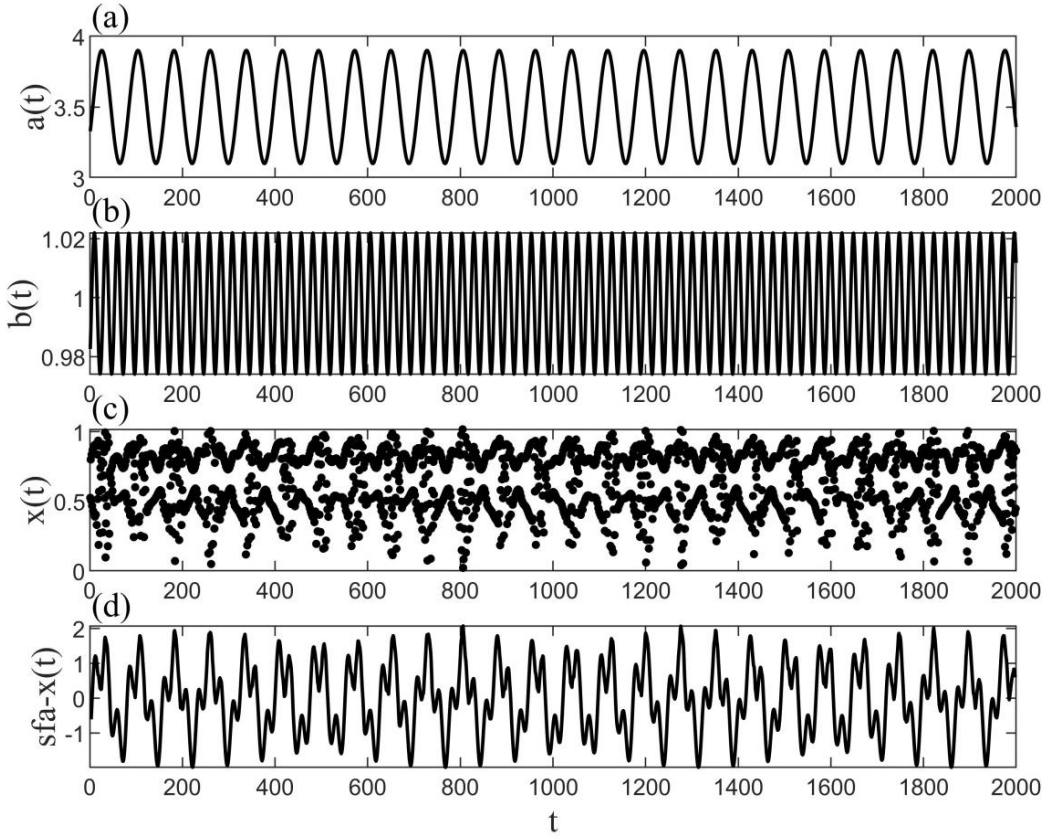

Figure 1s The time series of the parameters in the Logistic map with two-level structure. (a) Time series of true driving forces $a(t)$; (b)Time series of true driving force $b(t)$; (c) The non-stationary time series $x(t)$, which is controlled by $a(t)$and $b(t)$; (d) The slow feature $sfa\text{-}x(t)$ derived from $x(t)$by using SFA (m = 6and t = 1).

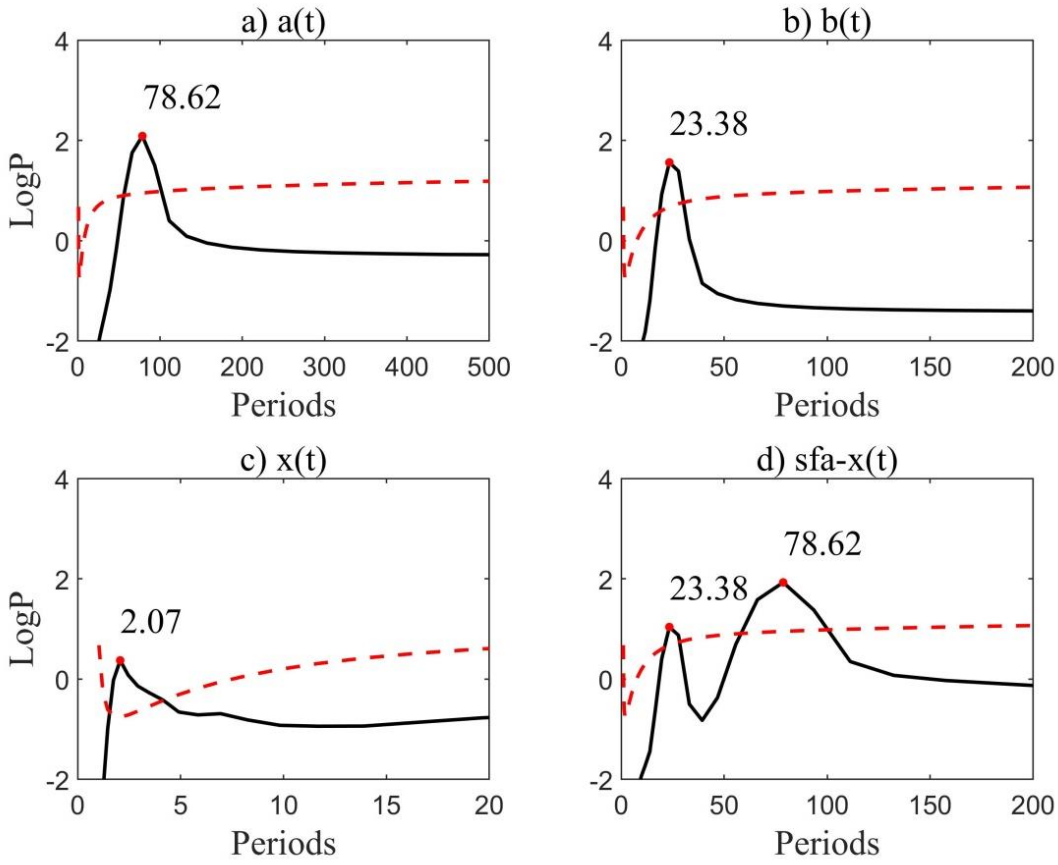

Figure 2s From (a) to (d) are the time-averaged power spectrums (black lines) of a(*t*), b(*t*), x(*t*) and sfa-x(t), respectively. The red dashed lines show the significant test at the significance level of 0.05 for wavelet analysis. The red dots indicate the peak periods that can pass the significant test. The values of corresponding period are denoted along with red dots.

m	Periods (reserve two decimal fractions)	
2	**23.38**	**78.62**
3	**23.38**	**78.62**
4	**23.38**	**78.62**
5	**23.38**	**78.62**
6	**23.38**	**78.62**
7	**23.38**	**78.62**
8	**23.38**	**78.62**
9	**23.38**	**78.62**
10	**78.62**	
11	**78.62**	
12	**78.62**	
13	**78.62**	
14	**78.62**	
15	**78.62**	
16	**78.62**	

Figure 3s The peak periods in the time-averaged power spectrum of SFA signals (significant at a significance level of 0.05) when setting different embedding dimensions (unit: step).

To sum up, based on a series of sensitivity test with an ideal model, we demonstrate the effectiveness and robustness of the technique of combining SFA with wavelet analysis. The sensitivity analysis of varying the embedding dimension appear so provide robust results: **The significant peak-periods of SFA signals can reflect the true driving forces very well. We note that other methods may be developed to quantify the uncertainties of the peak periods in future studies.**

Comment 2

Here are some additional facts that we are planning to add in order to connect our results to known dynamical mechanisms in decadal to multi-decadal variability. In this study, we identify four base periods in the driving signals of four climate modes as 2.32 yr, 3.90 yr, 6.55 yr and 11.02 yr, which are inferred to be associated with the signals of QBO, ENSO and sunspot cycle. Though they exhibit different coherent periods in the driving signals of different climate indices, our results provide some clues for the intricate relationships between driving forces and their harmonics in the variability of major climate modes as well as their coupling ways.

Recent studies on complex climate networks provided new insights into how the collective behavior of major climate modes affects global temperature variations (Tsonis et al., 2007; Tsonis 2018). By considering a network of major climate modes (more or less the same set as here and the theory of synchronized chaos, these previous studies found that the network may synchronize temporally. During synchronization, the increased coupling strength among the climate modes may lead to the destruction of the synchronized state that leads to changes in the trends of global temperature and the amplitudes of ENSO variability in decadal-to-multidecadal timescales. These studies proposed a dynamical mechanism and its related physical causes for the observed climate shifts. The idea that the interaction between major climate modes play a significant role in climate variability has in the last decade or so found many applications.

Solid dynamical arguments and past work offer a concrete picture of how the physics may play out (see G. Wang, K.L. Swanson, and A.A. Tsonis, 2009: The pacemaker of major climate shifts. Geophys. Res. Lett., doi:10.1029/2008GL03684 and references therein). NAO with its huge mass re-arrangement in north Atlantic affects the strength of the westerly flow across mid-latitudes. At the same time through its "twin", the arctic Oscillation (AO), it impacts sea level pressure patterns in the northern Pacific. This process is part of the so-called intrinsic mid-latitude northern hemisphere variability. Then this intrinsic variability through the seasonal "footprinting" mechanism couples with equatorial wind stress anomalies, thereby acting as a stochastic forcing of ENSO. Subsequently, ENSO with its effects on PNA can through vertical propagation of Rossby waves influence the lower stratosphere and in turn the stratosphere influence NAO through downward progression of Rossby waves. These results coupled with our results suggest the following 3-D super-loop NAO → PDO → ENSO → PNA → stratosphere → NAO, which may capture the essence of low-frequency variability in the northern hemisphere (Figure 4s).

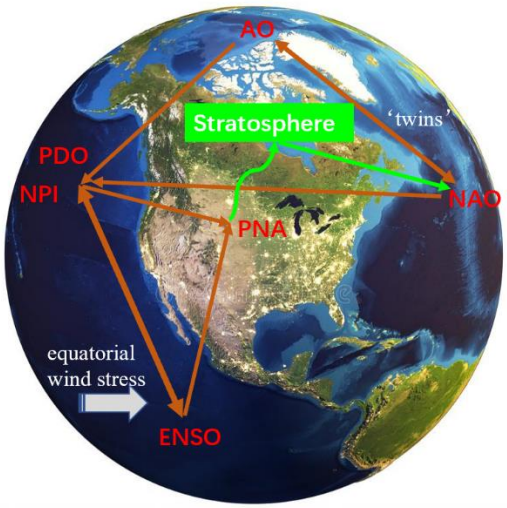

Figure 4s 3-D super-loop NAO → PDO → ENSO → PNA → stratosphere → NAO, which may capture the essence of low-frequency variability in the northern hemisphere.

Our results here provide additional possible players in picture above. Solar activity can be linked to stratosphere (see for example, Climate variability and sunspot activity: Analysis of solar influence on climate. Indrani Roy, Editor, Springer, ISBN 978-3-319-77106-9). Solar activity impacts the QBO and thus the stratosphere, which together with ENSO are implicated in this 3-D loop. Our results provide further new insights into those dynamical mechanisms and how the complex interactions among the base driving factors and their harmonics may cause the peak-periods in climate modes and thus affect climate variability.

We will make these points in the revised manuscript.